Atmos. Chem. Phys., 12, 6275–6289, 2012
www.atmos-chem-phys.net/12/6275/2012/
doi:10.5194/acp-12-6275-2012

Atmospheric Chemistry and Physics

Molecular hydrogen (H_2) combustion emissions and their isotope (D/H) signatures from domestic heaters, diesel vehicle engines, waste incinerator plants, and biomass burning

M. K. Vollmer[1], S. Walter[2], J. Mohn[1], M. Steinbacher[1], S. W. Bond[1], T. Röckmann[2], and S. Reimann[1]

[1]Empa, Swiss Federal Laboratories for Material Science and Technology, Laboratory for Air Pollution and Environmental Technology, Überlandstrasse 129, 8600 Dübendorf, Switzerland
[2]Institute for Marine and Atmospheric research Utrecht, Utrecht University, Princetonplein 5, 3508TA Utrecht, The Netherlands

Correspondence to: M. K. Vollmer (martin.vollmer@empa.ch)

Received: 30 January 2012 – Published in Atmos. Chem. Phys. Discuss.: 5 March 2012
Revised: 8 June 2012 – Accepted: 19 June 2012 – Published: 19 July 2012

Abstract. Molecular hydrogen (H_2), its stable isotope signature (δD), and the key combustion parameters carbon monoxide (CO), carbon dioxide (CO_2), and methane (CH_4) were measured from various combustion processes. H_2 in the exhaust of gas and oil-fired heaters and of waste incinerator plants was generally depleted compared to ambient intake air, while CO was significantly elevated. These findings contradict the often assumed co-occurring net H_2 and CO emissions in combustion processes and suggest that previous H_2 emissions from combustion may have been overestimated when scaled to CO emissions. For the gas and oil-fired heater exhausts, H_2 and δD generally decrease with increasing CO_2, from ambient values of $\sim$0.5 ppm and $+130$ ‰ to 0.2 ppm and -206 ‰, respectively. These results are interpreted as a combination of an isotopically light H_2 source from fossil fuel combustion and a D/H kinetic isotope fractionation of hydrogen in the advected ambient air during its partial removal during combustion. Diesel exhaust measurements from dynamometer test stand driving cycles show elevated H_2 and CO emissions during cold-start and some acceleration phases. While H_2 and CO emissions from diesel vehicles are known to be significantly less than those from gasoline vehicles (on a fuel-energy base), we find that their molar H_2/CO ratios (median 0.026, interpercentile range 0.12) are also significantly less compared to gasoline vehicle exhaust. Using H_2/CO emission ratios, along with CO global emission inventories, we estimate global H_2 emissions for 2000, 2005, and 2010. For road transportation (gasoline and diesel), we calculate 8.3 ± 2.2 Tg, 6.0 ± 1.5 Tg, and 3.8 ± 0.94 Tg, respectively, whereas the contribution from diesel vehicles is low (0.9–1.4 %). Other fossil fuel emissions are believed to be negligible but H_2 emissions from coal combustion are unknown. For residential (domestic) emissions, which are likely dominated by biofuel combustion, emissions for the same years are estimated at 2.7 ± 0.7 Tg, 2.8 ± 0.7 Tg, and 3.0 ± 0.8 Tg, respectively. For biomass burning H_2 emissions, we derive a mole fraction ratio $\Delta H_2/\Delta CH_4$ (background mole fractions subtracted) of 3.6 using wildfire emission data from the literature and support these findings with our wood combustion results. When combining this ratio with CH_4 emission inventories, the resulting global biomass burning H_2 emissions agree well with published global H_2 emissions, suggesting that CH_4 emissions may be a good proxy for biomass burning H_2 emissions.

1 Introduction

The atmospheric budget of molecular hydrogen (H_2) has recently gained increasing interest because of the ongoing discussion of a potential shift from our fossil fuel-based energy economy, to one that is based on H_2 as an energy carrier. Such a shift could lead to increased anthropogenic emissions from leakage of H_2, and therefore potentially change the chemistry and physics of our atmosphere (Schultz et al., 2003; Warwick et al., 2004; Vogel et al., 2012). A better understanding of the current anthropogenic contribution to the

atmospheric H_2 budget is a prerequisite for an assessment of potential future human impacts on the atmospheric H_2 cycle.

H_2 is abundant in the atmosphere at an average dry air mole fraction of ∼0.5 ppm (parts-per-million, µmole mole^{-1}) with a seasonality and an inter-hemispheric gradient both driven by the source and sink patterns. The atmosphere has not shown any significant H_2 trend over the past 15 yr (Grant et al., 2010b).

The atmospheric budget of H_2 is characterized by several major sources and sinks (Table 1). Their estimated quantities are highly uncertain as seen in the large ranges reported in the literature (Novelli et al., 1999; Hauglustaine and Ehhalt, 2002; Sanderson et al., 2003; Rhee et al., 2006b; Price et al., 2007; Xiao et al., 2007; Ehhalt and Rohrer, 2009; Pieterse et al., 2011; Yver et al., 2011). The sources are dominated by the atmospheric photochemical production of H_2 through dissociation of methane (CH_4) and non-CH_4 hydrocarbons (30–77 Tg yr^{-1}), fossil fuel combustion and other anthropogenic emissions (11–20 Tg yr^{-1}), and biomass and biofuel burning (13–20 Tg yr^{-1}). Microbially-induced H_2 emissions from N_2 fixation on land and in the oceans are estimated at 0–6 Tg yr^{-1} and 3–6 Tg yr^{-1}, respectively. There is also some evidence of abiotic H_2 release from plant litter although the mechanisms and global magnitude of this potential source are currently not fully understood (Derendorp et al., 2011; Lee et al., 2012). The dominant sinks are the enzymatic removal of H_2 by soil (55–88 Tg yr^{-1}) and the atmospheric removal through reaction with OH (15–19 Tg yr^{-1}). The atmospheric lifetime is estimated at 1.4–2 yr (Novelli et al., 1999; Simmonds et al., 2000; Rhee et al., 2006b).

The deuterium/hydrogen (D/H) ratio is a useful tool to study the atmospheric H_2 budget. Due to the large mass difference of 50 % between HH and HD, the isotopic signatures of the sources differ largely from one another, and the sink processes show relatively strong fractionations (Table 1). Isotope studies have revealed large deuterium enrichment in the stratosphere (Rahn et al., 2003; Röckmann et al., 2003; Rhee et al., 2006a), which is a consequence of the strong isotope fractionation in H_2 removal and relatively D-enriched H_2 that is formed photochemically from CH_4 (Gerst and Quay, 2001; Feilberg et al., 2007; Röckmann et al., 2010b; Nilsson et al., 2007, 2010). On the other hand, surface sources emit H_2 that is very depleted in D (Gerst and Quay, 2001; Rahn et al., 2002b,a; Röckmann et al., 2010a; Vollmer et al., 2010; Walter et al., 2011). These findings have helped to better constrain and understand the global H_2 budget in combination with ground-based D/H observations and chemical-transport models (Rice et al., 2010; Batenburg et al., 2011; Pieterse et al., 2011).

Combustion of fossil fuel is believed to be the major source of anthropogenic H_2 emissions (e.g. Ehhalt and Rohrer, 2009). Most of the global estimates (Table 1) are derived indirectly by using emission ratios of H_2 to carbon monoxide (CO) and combining these with CO emission inventories. This approach is based on the assumption that both H_2 and CO are products of incomplete combustion and that a constant intrinsic relationship exists between the two compounds (e.g. based on the water-gas shift reaction). Recognizing that most of the anthropogenic emissions stem from road transport-based fossil fuel combustion, some studies have distinguished between vehicular and non-vehicular emissions. Novelli et al. (1999) derived transportation-based emissions of 5–20 Tg yr^{-1} and non-vehicular emissions of 0.4–6 Tg yr^{-1}, resulting in a global estimate of 15 ± 10 Tg yr^{-1}. Ehhalt and Rohrer (2009) derived mean values of 8.6 Tg yr^{-1} for traffic emissions and 2.3 Tg yr^{-1} for non-traffic emissions, resulting in 11 ± 4 Tg yr^{-1}. Global traffic emissions were also estimated by Vollmer et al. (2007) using multiple methods and resulted in 5–11 Tg yr^{-1} in 2000 and decreasing to 3–5.5 Tg yr^{-1} by 2010. Bond et al. (2011a) estimate a decrease of H_2 emissions from road transportation from 4.5 Tg in 2010 to 2.3 Tg in 2020. Emissions from diesel-powered vehicles are much smaller compared to gasoline-powered vehicles because of different engine technology.

Driven by the CO ratio approach, recent studies have been conducted to better understand the $\Delta H_2/\Delta CO$ ratios in fossil fuel combustion, where the Δ denotes the enhancement over background expressed as mole fractions. A

Table 1. Global sinks and sources of tropospheric molecular hydrogen (H_2) and their isotope signatures[a].

	Strength[b] [Tg yr^{-1}]	isotope signature [‰ VSMOW[d]]
Sources		
Fossil fuel combustion	11–20	-196[e] to -270[f]
Biomass and biofuel burning	8[c]–20	-90[g] to -290 ± 60[e]
Photochemical production		+130 to +340[h]
from methane	15–26	$+190 \pm 50$[i] to $+213^{+264}_{-228}$
from VOC	10–18	–
Biological production		-628[j] to -741[l]
Land N_2 fixation	0–6	
Oceanic N_2 fixation	3–6	
Total Sources	47–96	
Sinks		kinetic isotope fractionation factors
Soil deposition	55–88	0.943 ± 0.024[e]
Reaction with OH	15–19	0.568[k]
Total Sinks	70–107	

[a] These estimates result in a tropospheric H_2 burden of 136–172 Tg, a mean isotopic composition of 120–132 ‰, and a tropospheric lifetime of 1.4–2 yr. [b] Ranges from the works of Novelli et al. (1999), Hauglustaine and Ehhalt (2002), Sanderson et al. (2003), Rhee et al. (2006b), Price et al. (2007), Xiao et al. (2007), Ehhalt and Rohrer (2009), Pieterse et al. (2011), and Yver et al. (2011) [c] Lower value from this work for the year 2000. [d] Referenced to Vienna Standard Mean Ocean Water (VSMOW). [e] From Gerst and Quay (2001). [f] From Rahn et al. (2002b). [g] From Rhee et al. (2006b). [h] Range from works of Gerst and Quay (2001), Rahn et al. (2003), Röckmann et al. (2003), Rhee et al. (2006b), Price et al. (2007), and Mar et al. (2007). [i] From Rhee et al. (2006a). [j] Rice and Quay, unpublished results. [k] From Sander et al. (2006) based on Ehhalt et al. (1989) and Talukdar et al. (1996). [l] From Walter et al. (2011).

fleet-integrated traffic tunnel study in Switzerland revealed a mean $\Delta H_2/\Delta CO$ of 0.48 (Vollmer et al., 2007), and a $\Delta H_2/\Delta CO$ of 0.45 was found from samples taken close to traffic exhaust in Germany (Hammer et al., 2009). Several recent studies of atmospheric H_2 and CO in Europe have also been used to derive anthropogenic urban $\Delta H_2/\Delta CO$ (Steinbacher et al., 2007; Hammer et al., 2009; Aalto et al., 2009; Yver et al., 2009; Bond et al., 2011b; Grant et al., 2010a; Popa et al., 2011), whereas some of these studies focused on traffic emissions by selectively analyzing the periods of rush-hour traffic. In order to derive a pure emission ratio, a correction of the measured $\Delta H_2/\Delta CO$ was proposed by Hammer et al. (2009) to remove the influence of the soil sink. The observed $\Delta H_2/\Delta CO$ increased from 0.33–0.43 to a narrow 0.47–0.49 in those urban studies, that have applied this correction (Hammer et al., 2009; Aalto et al., 2009; Yver et al., 2009). This is in close agreement with the results from the tunnel study (Vollmer et al., 2007). However, slightly higher $\Delta H_2/\Delta CO$ (without soil correction) have also recently been observed for the Bristol (United Kingdom) area by Grant et al. (2010a) (0.57 ± 0.06) and from the Cabauw tall tower in the Netherlands by Popa et al. (2011) (0.54 ± 0.07). Ehhalt and Rohrer (2009) found a different explanation for the lower observed urban $\Delta H_2/\Delta CO$ (compared to the traffic signal of $\sim$0.5) than Hammer et al. (2009). They argue that the differences in lifetimes (essentially the rapid H_2 removal by soil) is negligible in suburban observations, and explain the lower observed urban ratios (compared to pure traffic) as a mixture of the pure traffic signal with an unspecified non-traffic fossil fuel source characterized by a $\Delta H_2/\Delta CO$ of 0.2.

Combustion of biofuel and biomass is another significant source of H_2 to the atmosphere. The two combined combustion contributions were found to range between 13 and 20 $Tg\,yr^{-1}$ (see summary by Ehhalt and Rohrer, 2009). Price et al. (2007) distinguished between biomass ($10.1\,Tg\,yr^{-1}$) and biofuel ($4.4\,Tg\,yr^{-1}$) combustion. Of their $15\,Tg\,yr^{-1}$ H_2 emissions from biomass burning, Ehhalt and Rohrer (2009) assign $4.8\,Tg\,yr^{-1}$ to biofuel. Biomass burning emissions (excluding biofuel) are also estimated by Yver et al. (2011) at $7.8\,Tg\,yr^{-1}$ for mid-2006 to mid-2009. H_2 emissions from biomass burning are also given by the Global Fire Emissions Database version 3 (GFED3, data set at http://www.globalfiredata.org/, see also Giglio et al., 2010 and van der Werf et al., 2010). These estimates were made for 1997 to 2010 ranging 5.3–12.6 $Tg\,yr^{-1}$ with a mean of $7.8\,Tg\,yr^{-1}$. Various methods are used in the literature to derive the emissions for biomass and biofuel burning, including the scaling of H_2 to the amount of biomass burnt, to CO or CO_2, or using an isotope budget analysis (see Ehhalt and Rohrer (2009) for a summary). The H_2/CO from biomass burning has persistently been found to be lower compared to traffic combustion. Biomass burning field and laboratory studies typically show $\Delta H_2/\Delta CO$ of 0.15–0.45 with the majority of the published data in the narrow range of 0.2–0.3 (Crutzen et al., 1979; Cofer III et al., 1989, 1990, 1996; Ward et al., 1992; Laursen et al., 1992; Yokelson et al., 2009; Röckmann et al., 2010a; Yokelson et al., 2011).

The present study aims to improve our understanding of the anthropogenic H_2 emissions and their isotopic signature. We have experimentally investigated various potential anthropogenic H_2 sources. To our knowledge, these are the first published measurements of H_2 in the exhaust of residential heaters and waste incinerator plants. A revision of the global H_2 emissions from combustion is suggested, including fossil fuel, biofuel, and biomass combustion. For the latter, we use H_2/CO with updated biomass burning CO emissions and compare this approach with a new one based on H_2/CH_4. Finally, temporal changes in these emissions are addressed, a topic that has so far received little attention in the literature.

2 Methods

2.1 Residential fossil fuel and wood heater

Exhaust samples from residential oil, gas, and wood burners were collected in December 2008 and January 2009 in Switzerland from 9 roof-top chimneys and exhaust pipes (see Supplement for more details on the sampling and analysis). With the exception of the open wood fire, all heater systems are designed to heat a water reservoir of a closed-water cycle that distributes the heat through the buildings by means of hot water radiators or hot water floor heating systems. The samples were drawn through PFA tubing and transferred into 2 l glass flasks (NORMAG, Illmenau, Germany), fitted with 2 stopcocks, by means of a membrane pump (model N86-KTE, KNF Neuberger, Switzerland) to pressures of 1.8 bar. A drying cartridge containing magnesium perchlorate ($Mg(ClO_4)_2$) was fitted downstream of the pump to remove H_2O from the samples in order to avoid isotopic exchange between H_2 and H_2O during storage of the samples. The samples were stored in the dark and at room temperature before analysis on various instruments.

The samples were taken from a large variety of burner types, fuel systems, and burning capacities. If not specified differently in the Supplement, two samples (A and B) were taken at the same location, typically $\sim$5 min apart (Table 2). The sample pairs S-1 and S-2 were taken from oil burners of single-family houses. A variety of natural gas burners were also sampled (S-3 to S-7) ranging from single-family houses to larger building complexes. In addition to the fossil fuel-based heating systems, two wood-burning systems were sampled. The samples S-8 were taken from a modern (2007) fully automated wood-pellet burning system of a 2-family house. The samples S-9 were taken from an indoor open fire place of a single family house, in which pieces of local beech were burnt. The samples were drawn through an opening in the chimney system $\sim$4 m above the fire. Finally, ambient air samples were also collected during this and the waste incinerator campaign in order to determine

Table 2. Molecular hydrogen (H_2), its isotopic composition (δD), carbon monoxide (CO), carbon dioxide (CO_2), and methane (CH_4) in the exhausts of oil (O), gas (G) and wood (W) heaters, waste incinerators (I), and from ambient air samples (A). The incinerator samples are from 7 different incinerators (some measurement campaigns were repeated, hence 9 sets listed) and collected using discrete flask/bag or integrated (1 week) samples. S-Air and I-Air samples are ambient air samples collected during the study. Mole fractions (dry air) are given in ppm (10^{-6}) for H_2, CO, and CH_4, and in percent (10^{-2}) for CO_2. For δD, see text.

Sample	Type	building and sampling details	H_2 [ppm]	δD [‰]	CO [ppm]	CO_2 [%]	CH_4 [ppm]
S-1A	O	one-party house, burner startup	0.527	−25.6	10.7	6.33	1.17
S-1B	O	one-party house, optimal combustion	0.455	−34.7	7.01	6.10	1.20
S-2A	O	one-party house, optimal combustion	0.204	−52.3	4.59	10.2	0.54
S-2B	O	one-party house, optimal combustion	0.187	−139	3.70	10.2	0.54
S-3A	G	four-party apartment building, optimal combustion	0.403	−22.3	2.42	4.60	1.04
S-3B	G	four-party apartment building, optimal combustion	0.397	−17.8	2.37	4.47	1.05
S-4A	G	25-party apartment building, status of burner not known	0.389	63.7	0.95	2.95	1.48
S-4B	G	25-party apartment building, status of burner not known	0.638	30.9	3.04	0.15	20.1
S-5A	G	school, burner system A, old style	0.222	−206	15.4	8.89	0.19
S-5B	G	school, burner system B, H_2O condensation system	0.582	25.0	0.44	0.18	22.1
S-6A	G	large institution, optimal combustion	0.413	−103	2.43	10.6	0.00
S-6B	G	large institution, optimal combustion	0.400	−108	2.47	10.6	0.03
S-7A	G	one-party house, optimal combustion	3.36	−169	25.6	9.23	37.6
S-7B	G	one-party house, optimal combustion	3.39	−167	25.5	8.85	43.1
S-8A	W	two-party house, wood pellet heater, burner startup	20.6	−47.9	583	7.31	5.19
S-8B	W	two-party house, wood pellet heater, optimal burning	6.65	−182	69.5	8.74	1.26
S-9A	W	one-party house, open fire place, slow burning/reduced air draft	120	−204	699	2.92	49.2
S-9B	W	one-party house, open fire place, fast burning/strong air draft	381	−87.2	4090	3.35	102
S-Air	A	during above sampling period	0.551	55.9	0.32	0.05	1.99
I-1A	I	discrete sample	0.383	−229	7.54	8.80	–
I-1B	I	discrete sample	0.344	−308	7.54	8.80	–
I-1C	I	discrete sample	0.367	–	5.03	9.60	–
I-1D	I	discrete sample	0.616	−357	4.05	9.70	–
I-1E	I	discrete sample	0.341	–	–	–	–
I-2A	I	discrete sample	1.99	−173	30.6	9.40	–
I-2B	I	discrete sample	2.11	−165	30.6	9.40	–
I-2C	I	discrete sample	2.35	–	32.0	9.60	–
I-2D	I	discrete sample	2.05	−192	32.0	9.60	–
I-2E	I	discrete sample	1.92	–	31.1	9.60	–
I-2F	I	discrete sample	2.20	−157	31.1	9.60	–
I-3A	I	integrated sample	0.591	–	5.81	9.99	0.40
I-4A	I	integrated sample	4.71	–	9.97	9.51	1.20
I-4B	I	integrated sample	0.250	–	3.08	9.57	<0.40
I-4C	I	integrated sample	0.270	–	3.39	9.72	<0.40
I-5A	I	integrated sample	3.450	–	3.35	9.80	<0.40
I-5B	I	integrated sample	4.720	–	9.14	9.42	1.16
I-6A	I	integrated sample	0.863	–	11.4	9.87	<0.40
I-6B	I	integrated sample	0.668	–	11.6	9.70	<0.40
I-6C	I	integrated sample	0.726	–	12.8	10.2	<0.40
I-7A	I	integrated sample	0.265	–	5.55	9.59	<0.40
I-7B	I	integrated sample	0.375	–	3.78	9.19	<0.40
I-7C	I	integrated sample	0.268	–	3.95	9.49	<0.40
I-8A	I	integrated sample	0.677	–	6.72	10.3	<0.40
I-8B	I	integrated sample	0.742	–	6.45	10.2	<0.40
I-8C	I	integrated sample	4.75	–	11.1	10.4	0.76
I-9A	I	integrated sample	0.593	–	8.14	10.1	0.47
I-9B	I	integrated sample	0.574	–	7.41	10.0	0.43
I-9C	I	integrated sample	0.618	–	6.28	9.93	<0.40
I-Air1	A	during S-1 sampling	0.499	88.0	0.20	–	<0.40
I-Air2	A	during S-1 sampling	0.529	19.6	0.18	–	<0.40

approximate mole fractions of the air drawn for the combustion (Table 2).

The samples were measured at Empa for H_2 and CO in February 2009, using a gas-chromatograph (GC) with a reduction gas analyzer (RGA-3, Trace Analytical) based on mercuric oxide (HgO) reduction and UV light absorption by mercury (Vollmer et al., 2007; Bond et al., 2011b). The instrument is controlled through software for air monitoring (GCWerks, USA) and includes a correction for nonlinear system behavior (Vollmer et al. (2007); Bond et al. (2011b), details are also given in the Supplement). The measurements of flask samples were bracketed by the analysis of a working standard that allowed quantification and short-term instrumental drift correction. This working standard was referenced against the Max Planck Institute (MPI)-2009 primary calibration scale for H_2 (Jordan and Steinberg, 2011). The CO measurements were linked in a similar way to the NOAA/ESRL WMO-2000 calibration scale for CO. The mean measurement precisions were 0.6 % for H_2 and 0.4 % for CO (as determined from repeated analyses). The overall accuracies, including calibration scale and nonlinearity uncertainties, are estimated at ~ 5 % for both H_2 and CO. Some of the samples' H_2 and/or CO exceeded the detector's response or the range characterized for nonlinear system behavior. These samples were diluted using synthetic air, from which traces of H_2 and CO were removed using a catalyst (Sofnocat 514, Molecular Products, Thaxted, UK). Following dilution, some CO mole fractions were still above the upper limits of the range characterized and corrected for nonlinearity. Rather than applying these results we have used the measurements on other instruments (see below).

The samples were also analyzed (May 2009) on a GC (Agilent Technologies 6890N and controlled through GCWerks) equipped with a flame-ionization detector (FID) for CO and CH_4. This instrument has linear detector response in the ambient mole fraction range as found through earlier experiments (Steinbacher and Vollmer, unpubl. data). For the present work, measurements of two high mole fraction standards (2.01 ppm and 8.25 ppm, traced back to NIST SRM (Standard Reference Material) 2612a) revealed a slight CO nonlinearity at higher mole fractions, for which we corrected. The measurement precisions were 0.2 % for CH_4 and 1.1 % for CO. CO measurements are reported on the WMO-2000 calibration scale (with NIST and WMO-2000 in very close agreement, Zellweger et al., 2009) and CH_4 measurements are reported on the NOAA-2004 calibration scale (Dlugokencky et al., 2005). The overall accuracies, including calibration scale and nonlinearity uncertainties, are estimated at ~ 2 % for both compounds.

In order to quantify CO_2 and high mole fraction CO in the exhaust samples, most samples were also analyzed by Fourier Transform Infrared (FTIR) spectroscopy applying a spectrometer (Nicolet Avatar 370 InSb, Thermo Nicolet Corp., USA) equipped with a heated (40 °C) low-volume (50 ml) flow-through gas cell with 1m path-length (Model LFT-210, Axiom Analytical Inc., USA). Infrared spectra with 0.5 cm^{-1} optical resolution were recorded integrating over 128 spectral scans and trace gas mole fractions were retrieved by classical least square fitting in selected wavelength regions (Mohn et al., 2008). Calibration spectra were recorded under identical instrumental and spectroscopic conditions from certified and diluted calibration gases or by continuous injection of liquids into nitrogen. The expanded standard uncertainty (1σ) for CO_2, CO, and CH_4 is ~ 5%.

H_2 mole fractions and stable isotope D/H analysis of H_2 were conducted in March 2009 at the isotope laboratory of the Institute for Marine and Atmospheric research Utrecht (IMAU), Utrecht University, using isotope ratio mass spectrometry (Rhee et al., 2004). We report the isotope measurements using the "delta" notation, $\delta D = [(D/H)_s/(D/H)_{VSMOW} - 1] \times 1000$ ‰, where s refers to the sample and VSMOW is Vienna Standard Mean Ocean Water used as reference (Craig, 1961; Gonfiantini, 1978). The mean absolute 1-σ precision is estimated at 4.5 ‰ (Batenburg et al., 2011).

As described in the previous paragraphs, H_2, CO, and CH_4 were measured on several instruments. For those measurements that qualified for a comparison (within nonlinearity ranges, well above detection limits), we found an agreement within a few percent for the various measurement techniques, even though many results were slightly outside the combined (1σ) measurement precisions. For the final values used in our analysis, we have selected measurements from individual instruments or averages from two or more instruments. The selection was mainly based on choosing the measurements within the well-characterized nonlinearity ranges (RGA-3) and by excluding some low-mole-fraction CH_4 FTIR measurements for which more uncertainty was expected.

2.2 Waste incinerators

Exhaust gas was sampled at six waste incinerator facilities throughout Switzerland. These incinerators are equipped with one to four boilers and a sequence of catalysts and filters to remove most particles and toxic substances. These incinerators are designed for the combustion of household and industrial waste on a regional scale with yearly waste throughputs of typically 90 000–220 000 t. The plants I-1 and I-2 were sampled in 2008. A large set of incinerators was sampled from September to December 2010 through collection of integrated (1 week) dried (MD-070-24S-4, Perma Pure, USA) exhaust gas samples in Cali-5-Bond™ sampling bags (GSB-P/44, Ritter Apparatebau, Germany). They were analyzed by FTIR spectroscopy for CO, CO_2, and CH_4. For H_2 and CO analysis, some of these Tedlar bag samples were cryogenically transferred into evacuated stainless steel flasks, which were immersed in liquid nitrogen. This was necessary to create samples with super-ambient pressure, which is required due to our RGA instrumental design. Samples with CO mole fractions above 1.5 ppm were transferred directly

from the Tedlar bags into a small (50 ml) evacuated stainless steel container, immediately diluted (and pressurized) with purified (H_2 and CO free) synthetic air, and subsequently analyzed on the RGA-3.

The incinerator exhaust gas samples were stored in Tedlar bags for less than two weeks before transfer and/or analysis. In order to assess potential diffusive exchange/loss of H_2 through the Tedlar bags during storage, a stability experiment was conducted that demonstrated sufficient storage stability over the course of our storage period. However, our experiments showed significant enhancement of H_2 and CO over a longer storage period (see Supplement).

2.3 Diesel-powered vehicles

Exhaust gas analysis from diesel-powered vehicles was conducted at Empa in 2008 as part of an extensive dynamometer test stand emission study that included H_2 emissions, and that were part of a larger fleet study also including gasoline vehicles (Bond et al., 2010; Bond, 2010). This included measurements of 5 light-duty diesel delivery vehicles and 1 diesel passenger car, most of which were tested under 6 different driving cycles. All diesel vehicles were classified by the Euro-4 emission standard. All vehicles were equipped with oxidation catalysts and three had diesel particle filters. On-line direct exhaust measurements were conducted for a suite of compounds. H_2 was measured using an on-line mass spectrometer (H-sense, V&F Analyse- und Messtechnik GmbH, Austria, see Bond et al. (2010) for a description of the instrument) and CO was measured using Mexa 7100 AIA-721A and AIA-722 instruments (Horiba, Japan). The data used here are from the periods of large H_2 and CO mole fractions (up to several hundred ppm), which occurred during all cold starts and during some of the acceleration phases. Hence our results are based on periods of emissions selected for their high emissions and they include the investigation of the H_2/CO ratios, while the study by Bond et al. (2010) focused on the emission factors covering the entire driving cycles and did not include the H_2/CO ratio of diesel exhaust.

3 Results and discussion

3.1 H_2 and H_2/CO

In this paper, we will exclusively use the molar H_2/CO ratio and not the weight-based ratio, which is sometimes used in the literature (to convert from molar to weight-based to molar, divide by 14). Also, we will distinguish between the ratio based on measured mole fractions, here termed "absolute ratio", and the ratio calculated after subtraction of the background dry air mole fraction, which are typically found in the combustion intake air, i.e. $H_2 \approx 0.5$ ppm and $CO \approx 0.2$ ppm. We express the ratio for background corrected values in the Delta (Δ) notation ($\Delta H_2/\Delta CO$). This distinction is important for the discussion of the many low-mole-fraction measurements in the present study, but becomes negligible for high-mole-fraction source signals, when it is sometimes ignored in the following text. Analogously, we proceed with the molar ratio of H_2/CH_4 and $\Delta H_2/\Delta CH_4$, and use $CH_4 \approx 1.8$ ppm as a typical background mole fraction.

3.1.1 Residential fossil fuel heater

Our results are shown in Fig. 1 and listed in Table 2. Most of the heater exhaust samples (S-1 to S-6) exhibit surprisingly low H_2 mole fractions in the range 0.19–0.64 ppm, which is at or below the mole fractions of the ambient intake air ($\sim$ 0.5 ppm). Thus many of the sampled heaters are net sinks for H_2. In contrast, most heater samples have significantly elevated CO mole fractions (1–15 ppm) compared to the measured ambient air (0.2–0.3 ppm). Consequently, the absolute H_2/CO is small, typically 0.03 to 0.2 and even lower with some negative ratios (-0.1 to 0.13) when using the Δ notation (differences to background). As an exception, H_2 was significantly elevated in S-7 (3.5 ppm), a natural gas-fueled residential heater. For this heater, CO and CH_4 were also largely elevated (Table 2), suggesting that the burner of this heater may not have been adjusted properly.

3.1.2 Residential wood heater

In contrast to the oil and gas heater exhausts, both H_2 and CO are strongly elevated in the wood-based combustion samples, S-8, and S-9, with the highest H_2 mole fractions for the open wood fire place (S-9B, 390 ppm) during fast burning under a strong intake air draft. For the wood pellet heater, H_2 decreases from the starting phase of the burning (S-8A, 20.6 ppm) to the optimal burning phase (S-8B, 6.2 ppm) with similar air to fuel ratio for these two samples, as indicated by similar CO_2 mole fractions (Fig. 2). If we generally use CO_2 as a proxy for combusted fuel, then our results indicate that modern wood pellet combustion systems reduce H_2 and CO emissions compared to less controlled open fires, but that they are still much larger than oil and natural gas-fueled combustion systems.

3.1.3 Waste incinerators

Exhaust gas mole fractions from waste incinerators were generally low, with near ambient H_2 mole fractions (0.3–0.9 ppm) and enhanced CO mole fractions (3–13 ppm). This results in the absolute H_2/CO of typically 0.05–0.1 and virtually zero or negative in the Δ notation (Fig. 1). Given that the sampled waste incinerators are equipped with a suite of sequential filter systems including electrostatic filters and flue gas scrubbers, the observed H_2 and CO probably represent a strongly altered combustion signal. There are a few exceptions to the low-H_2 emissions. At plant I-2 much higher mole fractions of H_2 ($\sim$2 ppm) and CO ($\sim$30 ppm) were observed. This is likely a result of a poor adjustment of a natural gas heater for NO_x removal, which this plant had in operation

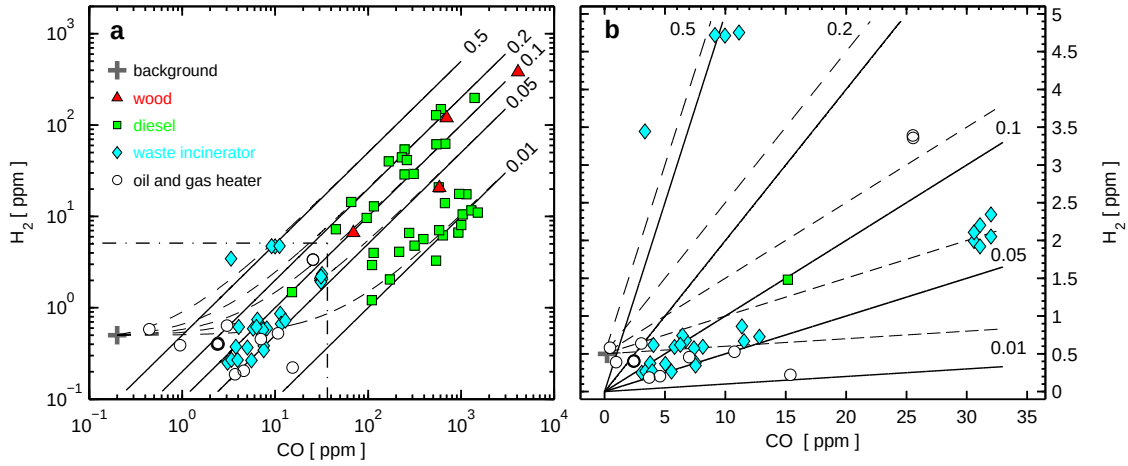

Fig. 1. Molecular hydrogen (H_2) versus carbon monoxide (CO) in combustion exhaust. All measurements are shown on a log-log scale in **(a)** and a selection (delimited by dashed-dotted box) on a linear scale in **(b)**. The H_2 and CO mole fractions in background air are shown as grey plus sign. Molar H_2/CO ratio lines are shown as visual guides with the origins set at background mole fractions (Δ ratio, backgrounds subtracted, see text) shown as dashed lines and at zero mole fractions (absolute ratios, no background subtraction) as solid lines.

(downstream of all filters) when our samples were collected. Additionally at three waste incinerators, individual weekly-integrated exhaust gas samples (I-4A, I-5B, I-8C) exhibited elevated H_2 ($\sim$ 4.8 ppm) and CO ($\sim$ 10 ppm), while two of the samples also showed enhanced CH_4 ($\sim$ 1.2 ppm) compared to all other plants (<0.5 ppm).

3.1.4 Diesel-powered vehicles

The dynamometer test stand on-line diesel exhaust measurement results shown in Fig. 1 are from the study of Bond et al. (2010), but limited to episodes selected for high H_2 and CO emissions. We find a median H_2/CO ratio of 0.026 (inter-percentile range 0.12, Fig. 1 and Supplement). The H_2/CO ratios observed for the diesel-powered vehicles are significantly smaller compared to those for gasoline-powered vehicles of 0.48 ± 0.12 found during a tunnel study (derived from the total fleet ratios by Vollmer et al., 2007) and of 1.0 (sub-cycle means of 0.48–5.7) determined from a laboratory study on vehicles using exclusively modern combustion and exhaust treatment technology (Bond et al., 2010). Hence not only are the CO emissions from diesel powered engines smaller compared to gasoline powered engines, but the H_2/CO ratios are also smaller, suggesting that the global H_2 emissions from traffic are even more dominated by the gasoline-powered vehicles than the CO emissions.

The lower H_2 and CO emissions and the lower H_2/CO for diesel exhaust compared to those of gasoline are most likely related to the different types of combustion. In a modern gasoline engine, the air-fuel ratio (expressed as λ) is set to near 1, where $\lambda < 1$ is fuel-rich (excess fuel) and $\lambda > 1$ is fuel-lean (excess oxygen). Under these conditions, the H_2 and CO are presumably strongly controlled by the the water-gas shift reaction, $CO + H_2O \leftrightarrow CO_2 + H_2$, and rapid isotopic exchange between H_2O and H_2 (Vollmer et al., 2010). In contrast, diesel is combusted at higher temperatures under fuel-lean conditions. It is likely that the oxidation of H_2 and CO by O_2 becomes an important sink for these two compounds, presumably with preferential removal of H_2 over CO thereby leading to the relatively low absolute H_2/CO.

3.2 Relationships between δD, H_2, and CO_2

The isotopic signatures D/H of the heater exhaust samples were generally found to be strongly depleted (Table 2), down to $\delta D = -206$ ‰, compared to ambient air levels ($\delta D \approx +130$ ‰, Gerst and Quay, 2001; Rhee et al., 2006b; Rice et al., 2010; Batenburg et al., 2011). These isotopic signatures and the H_2 mole fractions vs. CO_2 are shown in Fig. 2, along with the measurements from the waste incinerator exhaust samples. The δD and the H_2 mole fractions for the gas and oil heater samples both decrease with decreasing air-fuel ratio, represented by increasing CO_2 mole fractions. These results are difficult to interpret. At first glance, the decreasing H_2 mole fractions (to below ambient air mole fractions) suggest that some of the H_2 of the intake air is removed during the combustion. Interestingly, if we extrapolate the linear fit in Fig. 2 to the maximum possible CO_2 mole fractions of 21 % (all oxygen consumed), then the H_2 equals virtually zero (−0.002 ppm). However, such a removal process would most likely be associated with a normal (positive) kinetic isotope effect (KIE), as most chemical reactions are. Consequently the δD of the remaining H_2 should then increase. However, the opposite is observed, namely a strong depletion (reaching −325 ‰ if also linearly extrapolated to 21 % CO_2). Only an inverse KIE could explain the

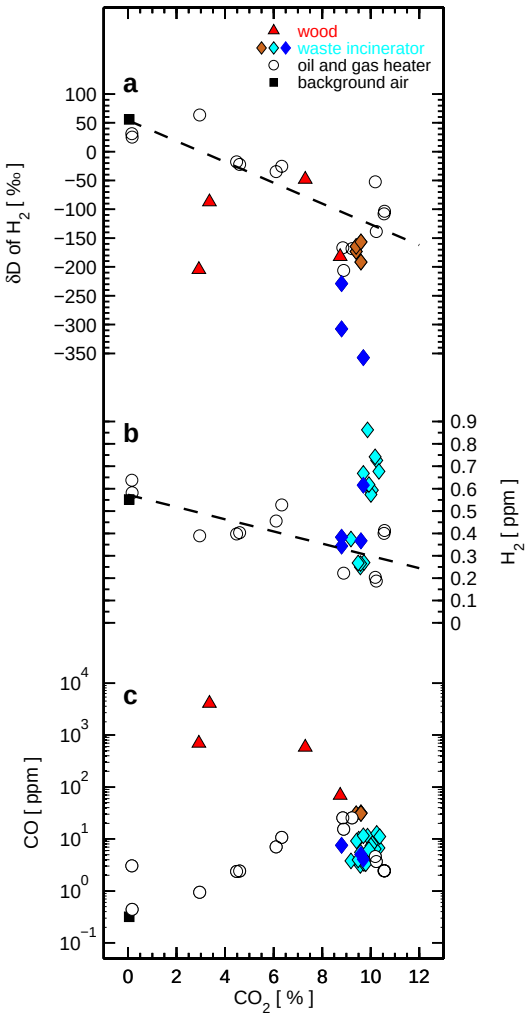

Fig. 2. Molecular hydrogen (H_2) isotopic composition (δD, **a**), H_2 **(b)** and carbon monoxide (CO, **c**) mole fractions versus carbon dioxide (CO_2) from residential heating combustion and waste incinerator plants. Not all waste incinerator measurements appear in all three subplots because they were either not measured or exceed the plotting range. Blue diamonds are for waste incinerator I-1, those in orange are for I-2, and those in cyan are from a later measurement campaign when no isotope measurements were conducted (I-3 to I-9). Samples with H_2 mole fractions >1 ppm (S7–S9, I-2, I-4A, I-5, I-8C) are omitted from **(b)** to better show the variability of the oil and gas heater measurements. The dashed lines are linear fits through the oil and gas heater measurements, excluding S-7. These fits are $\delta D = -18.052 \times CO_2 + 54.305$ for **(a)** and $H_2 = -0.0274 \times CO_2 + 0.5729$ for **(b)** and their respective units.

two observations of decreasing mole fractions and isotopic depletion. Inverse KIEs have been observed for catalyzed reactions involving hydrogen and carbon (e.g. Shi and Jin, 2011), but we were unable to find data on the KIE of H_2 combustion. As an alternative explanation, the observed strongly-depleted D/H could derive from the D/H in the fuel, for oil and natural gas generally contain strongly depleted D/H (e.g. Schimmelmann et al., 2006). However, if the hydrogen of the fuel was a significant contributor to the molecular hydrogen in the exhaust (and if there was no sink), then the H_2 mole fraction should increase with increasing CO_2 (i.e. with increasing amount of combusted fuel), which we do not observe. This leads us to suggest two explanations for the results from our measurements of heater exhausts. One explanation is removal with an inverse KIE, which we consider less likely. The other explanation is a concurrent production and removal processes – a source of H_2 (from the fuel) with significantly depleted D/H and a simultaneous removal of H_2 with a positive fractionation, which is, however, not large enough to compensate for the depleted D/H source.

The samples from wood fires show no obvious relationship between δD and CO_2 (Fig. 2) but generally their δD values are lower than those of the oil and gas burner samples. They show relatively high combustion efficiency (low molar (ppm / ppm) CO/CO_2 ratio, range $8 \times 10^{-4} - 0.12$) compared to other wood combustion results by Röckmann et al. (2010a).

A "Keeling plot" analysis, as is shown in Fig. 3, illustrates some of our findings on the H_2 mole fraction and the δD. In a simplified system with a single source (combustion) of hydrogen that mixes with ambient air, a linear relationship of δD vs. inverse H_2 mole fraction can be observed, which points to a specific end-member isotopic signature (at $1/H_2 = 0$). This is shown for the results of a study of H_2 in urban air in Los Angeles (Rahn et al., 2002a) and characterizes the road traffic exhaust. Our unique samples from one gas heater and one waste incinerator, both with poorly tuned combustion of natural gas, agree fairly well with this isotope mixing line. However, most oil and gas heater results and another set of waste incinerator samples (I-1) deviate from this mixing line and show a large spread of D/H, but all display relatively low H_2 mole fractions. The I-1 samples have the lowest δD observed during our study (−229 to −357 ‰). Our few wood samples with high H_2 mole fractions show a large δD variability and support a similar finding on wood combustion by Röckmann et al. (2010a), although two of our samples have significantly "heavier" δD compared to their study.

3.3 H_2/CH_4 from heaters, incinerators, and biomass burning

Our measurements of CH_4 in the different exhausts show highly variable mole fractions (Fig. 4). While the wood combustion samples exhibit mole fractions of up to 100 ppm, the heater samples and the waste incinerator samples show much lower mole fractions, and many of these are below the ambient air mole fractions of ≈2 ppm. These combustion processes are thus a net sink of CH_4. Wood combustion and waste incinerator samples have molar H_2/CH_4 ranging approximately 1–4. In contrast, most fossil fuel heater samples show ratios <1. In Fig. 4 we also show H_2/CH_4 from

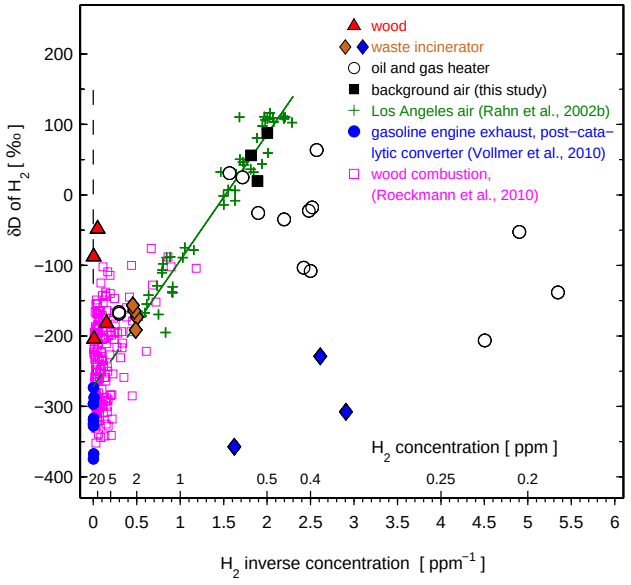

Fig. 3. Relationship of molecular hydrogen (H_2) isotopic composition (δD) versus inverse H_2 mole fraction ("Keeling plot") for samples from this study compared with results from Rahn et al. (2002a) with a green line fitted through their data, from Vollmer et al. (2010), and Röckmann et al. (2010a). Some of our samples are in fair agreement with the relationship found by Rahn et al. (2002a): these are the poorly-adjusted natural gas combustion burners from one waste incinerator plant (I-2, using natural gas post-filter combustion for NO_2 removal, shown as orange diamonds) and one residential heater. Most oil and gas heater and the waste incinerator samples I-2 (dark blue diamonds) show an opposite relationship, i.e. decreasing mole fraction for decreasing δD.

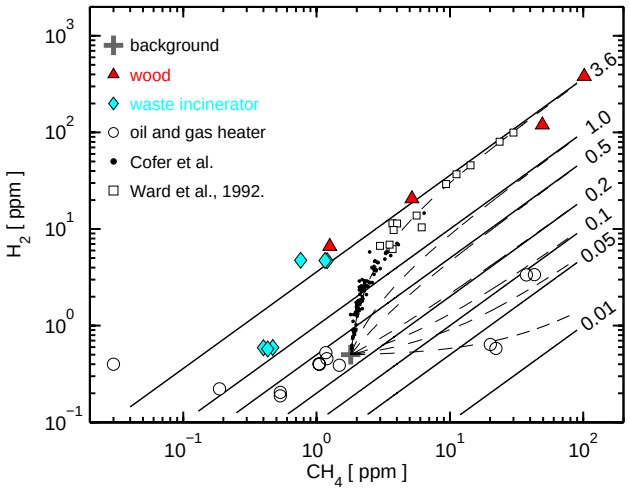

Fig. 4. Molecular hydrogen (H_2) versus methane (CH_4) in combustion exhaust. The measurements are shown on a log-log scale. Results from wildfires are from Cofer III et al. (1989, 1990, 1996) and Ward et al. (1992) and show a molar $\Delta H_2/\Delta CH_4$ ratio (background mole fractions subtracted) of 3.6 (weight based ratio 0.45). The H_2 and CH_4 mole fractions in background air are shown as grey plus sign. Molar H_2/CH_4 ratio lines are shown as visual guides with the origins set at background mole fractions (Δ ratio, backgrounds subtracted, see text) shown as dashed lines and at zero mole fractions (absolute ratios, no background subtraction) as solid lines.

a variety of wildfires (savanna, boreal forests, wetlands) and burning types (smoldering and flaming) from Cofer III et al. (1989, 1990, 1996) and Ward et al. (1992). To investigate the correlation between H_2 and CH_4 for these studies, we have subtracted the respective mean background mole fractions for each of the individual studies (as published along with the fire emission data) and linearly fitted the ΔH_2 vs. ΔCH_4. This results in $\Delta H_2/\Delta CH_4 = 3.61$ (corresponding to a weight-based ratio of 0.45) with 95 % confidence bounds 3.55–3.66 and $R^2 = 0.99$. Alternatively, a simple statistical averaging of all $\Delta H_2/\Delta CH_4$ yielded a ratio of 3.5 (1 stdv = 1.3). The $\Delta H_2/\Delta CH_4$ as calculated from emission factors from the open biomass burning studies by Yokelson et al. (2009) and Yokelson et al. (2011) agree well with our results, as they yield molar ratios of 4.32 ± 1.6 and 3.58 ± 1.4, respectively. Our wood fire exhaust measurements were not used to derive the above ratio, but they bracket this ratio with reasonable agreement. For the three high mole fraction samples, we find $\Delta H_2/\Delta CH_4$ of 2.5, 3.8, and 5.9 (listed with decreasing CH_4 mole fraction, Fig. 4). Interestingly, some of the low CH_4 mole fraction (below background values) samples (fourth wood sample and some incinerator samples) also support this ratio if their uncorrected (for background) ratios H_2/CH_4 were used instead of $\Delta H_2/\Delta CH_4$. From this analysis we conclude that for biomass burning, CH_4 emissions may be a good proxy for H_2 emissions.

3.4 Implications on global H_2 emissions from combustion

Global H_2 emissions from combustion can be estimated directly by using H_2 emission factors, which are related to the combusted material (e.g. dry-weight or carbon content), or by using combustion ratios to other trace gases (e.g. CO), and using their corresponding emission inventories. For H_2, our understanding of both approaches is currently incomplete. Our goal is to improve our understanding of the H_2/CO ratio approach (Table 3) and introduce the H_2/CH_4 approach. We estimate H_2 emissions from transportation, residential combustion (fossil fuel and biofuel), and biomass burning (Table 3). To deduce global emissions from H_2 combustion, we base our analysis mainly on the inventories by Fulton and Eads (2004), by the Emission Database For Global Atmospheric Research (EDGARv4.2) project (Olivier et al., 2002), and by GFED3. The EDGAR emission inventories are presumably based on the United Nations Framework Convention on Climate Change (UNFCCC) common reporting format (CRF) emission inventory – however, these lack emission information from many countries not reporting to UNFCCC.

Table 3. Molar [ppm / ppm] ratios of molecular hydrogen (H_2) to carbon monoxide (CO), to methane (CH_4), and isotopic signatures (δD-H_2) for selected combustion processes. Global H_2 emissions (in Tg) are given for 2000, 2005, and 2010.

	absolute H_2/CO	relative[a] $\Delta H_2/\Delta CO$	absolute H_2/CH_4	relative[a] $\Delta H_2/\Delta CH_4$	δD-H_2 [‰ VSMOW]	Global Emissions 2000	2005	2010
transportation								
gasoline, road	0.5[b]	0.[b]	–	–	-270 ± 50[d]	8.2 ± 2.1	5.9 ± 1.5	3.8 ± 0.94
diesel, road	0.026	$\leq$0.026	–	–	–	0.072 ± 0.036	0.063 ± 0.032	0.054 ± 0.027
waste incinerators	0.05–0.1	0	2 ± 1	<0	-250 ± 100	neg[g]	neg[g]	neg[g]
residential (domestic)								
oil and gas heaters	0.03–0.2	0	var[f]	var[f]	-100 ± 50	neg[g]	neg[g]	neg[g]
biofuel	0.25 ± 0.05[c]	0.25 ± 0.05[c]	3.6[c]	3.6[c]	-290 ± 60[e]	2.7 ± 0.7[h]	2.8 ± 0.7[h]	3.0 ± 0.8[h]
biomass	0.25 ± 0.05[c]	0.25 ± 0.05[c]	3.6[c]	3.6[c]	-290 ± 60[e]	5.7 ± 1.4[i]	8.4 ± 2.1[i]	9.4 ± 2.3[i]

[a] Ratio after subtraction of background mole fractions. [b] Based on works by Vollmer et al. (2007); Hammer et al. (2009). [c] Based on works by Cofer III et al. (1989, 1990, 1996); Ward et al. (1992); Laursen et al. (1992) and supported by this study. [d] Based on Rahn et al. (2002b) with uncertainty based on rough estimate using results by Vollmer et al. (2010). [e] Gerst and Quay (2001). [f] Highly variable, H_2/CH_4 ranges 0.03 to 13, $\Delta H_2/\Delta CH_4$ ranges -0.043 to 0.35. [g] Negligible compared to other H_2 combustion sources. [h] Based on EDGARv4.2 with the value for 2010 extrapolated from earlier years. [i] GFED3 (Giglio et al., 2010; van der Werf et al., 2010) with considerable inter-annual variability in the full 1997–2010 record.

3.4.1 Transportation emissions

Road transport CO emissions have been undergoing large declines in recent decades (Fulton and Eads, 2004) due to improved combustion and catalytic converter technology. Fulton and Eads (2004) estimate total (gasoline and diesel) global road traffic CO emissions to decline from 270 Tg in 2000, to 200 Tg, 135 Tg, and 90 Tg in 2005, 2010, and 2015, respectively. While the road diesel CO contribution was reported very small in the 1980s (6 Tg yr^{-1} vs 232 Tg yr^{-1} for gasoline, Duncan et al., 2007), its contribution relative to gasoline increased in the later years. Fulton and Eads (2004) estimate road traffic diesel CO emissions for the above-mentioned four years at $\sim$40 Tg, 35 Tg, 30 Tg, and 25 Tg, respectively (sum of only freight trucks and buses). Thus the relative contribution of CO emissions from diesel is steadily increasing, despite little change in the relative usage of the two fuel types, which are consumed in similar quantities (gasoline of 1.13×10^{12} vs. diesel of 0.87×10^{12} l gasoline-equ. for 2010, Fulton and Eads, 2004). These changes are likely due to the large improvements in gasoline combustion clean-up technologies. For H_2 traffic emissions, we use the above CO emission estimates by Fulton and Eads (2004) and combine these with approximated H_2/CO ratios. For gasoline, we use a H_2/CO ratio of 0.48 ± 0.12 based on the literature data (Vollmer et al., 2007; Hammer et al., 2009; Aalto et al., 2009; Yver et al., 2009). For diesel, we use a molar H_2/CO of 0.026 (corresponding to a weight-based ratio of 0.0018) from out test stand measurements (see Supplement). The differences of the CO emission estimates by Fulton and Eads (2004) to those by EDGAR (sector 1A3b, 206 Tg for 2000 and 155 Tg for 2005) suggest that there are significant uncertainties in the CO emissions. Due to lacking uncertainties in these data sets, we assign somewhat arbitrary errors of 25 % to our results for gasoline and 50 % for diesel. Results for the years 2000, 2005, and 2010 are given in Table 3 and show declining traffic H_2 emissions and increasing relative contributions from diesel, which however remain below 2 % of the total traffic emissions. Our estimates are in agreement with those derived by Vollmer et al. (2007) and Bond et al. (2011a). Our estimates on H_2 emissions from traffic are based on a temporally constant H_2/CO in the "average" world fleet. However, a recent study by Bond et al. (2010) suggests that the H_2/CO could increase significantly due to improving clean-up technologies (possibly to $H_2/CO \approx 1$). When calculating H_2 emissions from H_2/CO and using CO inventories, then this potential increase would have an opposite effect to the declining CO emissions. Thus it is possible that the global H_2 emissions from traffic may not decline as strongly in the near future as one would imply from our estimated 2000–2010 decline. We have neglected a potentially variable H_2/CO in our estimates because we have assumed that a potentially increasing H_2/CO is not significantly penetrating the "world" fleet so soon, and also argue that their overall CO contributions are less because these emissions with potentially enhanced H_2/CO are from modern vehicles with low CO emissions.

Diesel H_2 emissions are also expected to occur from diesel fuel use in water and rail transportation. According to Fulton and Eads (2004), the fuel use for these categories are roughly the same as for the sum of freight trucks and buses. However there is no information on H_2/CO for ship and train emissions. Ultimately, H_2 emissions are also expected to occur from diesel combustion for other purposes (e.g. power generation), but with poor understanding on CO emissions and H_2/CO ratios. We therefore exclude these categories from our analysis.

3.4.2 Domestic emissions (biofuel and fossil fuel)

The EDGAR CO inventory has one single highly-aggregated category "Residential and others" (1A4), which contains

both emissions from fossil fuel (oil, gas, coal) and biofuel. This makes it impossible to identify the component that is solely due to oil and gas emissions. The UNFCCC CRF divide their category 1A4 ("other sectors") into 3 subcategories, where 1A4b ("residential") CO emissions comprise the largest fraction of 1A4. By comparing the EDGAR and UNFCCC emissions with the study by Yevich and Logan (2003) on biofuel emissions, we conclude that the dominant fraction of residential CO emissions in the developing world is from biofuel. Surprisingly, in industrialized countries, biofuel CO emissions may also play an important role compared to other emissions in the 1A4 category, even though in these countries, a large fraction of the residential energy usage derives from fossil fuel heating systems, particularly in colder climate regions. The difficulty in extracting the various subtypes of emitters in this category 1A4b is that national emission inventories do not reach this level of detail in their UNFCCC CRF tables, and access to the relevant data from individual countries is difficult. For Switzerland for example, residential 1A4b emissions of CO are 45 kt yr^{-1} according to the UNFCCC CRF. However, the largest fraction ($\sim 80\,\%$) of these CO emissions derives from biofuel (wood) burning for heating (like the wood fire emissions of this study) and from seemingly minor applications ($\sim 8\,\%$), such as gardening tools (2-stroke engines) with very large CO emission factors (Leippert et al., 2010). The oil and gas heating systems' CO emissions for Switzerland are comparably small ($\sim 5\,\%$), despite their dominance from an energy perspective (Leippert et al., 2010). This example supports our conclusion that on a global basis, the majority of the CO emissions from the "residential" sector are from biofuel combustion and not from oil or gas combustion. On the basis of this finding, we adopt the biomass burning $\Delta H_2/\Delta CO$ of 0.25 ± 0.05 (Table 3), which we derive from the literature (see Introduction), to calculate these residential emissions. Our four wood burning measurements show a significantly lower $\Delta H_2/\Delta CO$ ratio (0.099 ± 0.057), but more studies are necessary to investigate a representative ratio from wood heating systems. H_2 emissions from oil and gas are likely insignificant given the near zero $\Delta H_2/\Delta CO$ emission ratios. CO emissions from residential coal combustion are likely small compared to biofuel emissions (the biofuel CO emissions by Yevich and Logan (2003) nearly match the total "residential" emissions in EDGAR). However, here we assume that the corresponding H_2 emissions are also small, i.e. that the H_2/CO ratio of coal combustion is not significantly larger than that of biomass combustion. The EDGAR global estimates for domestic CO emissions show a trend of increasing emissions with time, but with relatively little temporal variation, with a mean value of 153 ± 5 Tg yr^{-1} for 1980–2008 (Fig. 5 and Table 3). These convert to global H_2 emissions of 2.7 ± 0.09 Tg yr^{-1}. Here we omit using EDGAR CH_4 to derive H_2 emissions because in this sector, fugitive CH_4 emissions, presumably from leakage (with presumably insignificant corresponding H_2 emissions), contribute strongly to the total CH_4 emissions of this sector. Our estimated emissions for this sector are smaller (but probably within the combined uncertainties) compared to the 4.4 Tg yr^{-1} for biofuel by Price et al. (2007) and the 4.8 Tg yr^{-1} by Ehhalt and Rohrer (2009) for unspecified years.

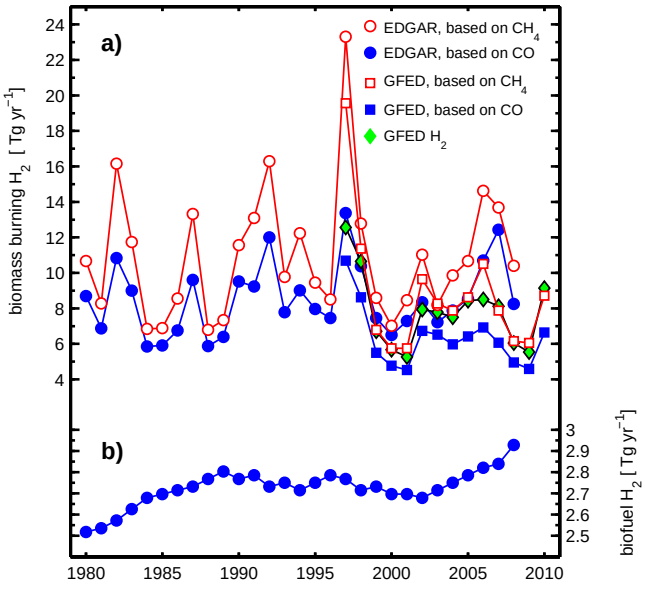

Fig. 5. Global molecular hydrogen (H_2) emissions from biomass burning **(a)** and domestic emissions (**b**, with finer y-axis resolution) using emission inventories from the Emission Database For Global Atmospheric Research (EDGARv4.2) project (Olivier et al., 2002), and the Global Fire Emissions Database version 3 (GFED3, data set at http://www.globalfiredata.org/, see also Giglio et al., 2010 and van der Werf et al., 2010). The carbon monoxide (CO) emission inventories were converted to H_2 using a molar H_2/CO ratio of 0.25, and the methane (CH_4) emission inventories were converted to H_2 using a molar H_2/CH_4 ratio of 3.6 (see text). GFED3 H_2 and CH_4-derived H_2 emissions agree well, while CO-derived H_2 emissions are considerably lower. EDGAR emissions are generally larger than GFED3 emissions.

3.4.3 Biomass burning

For biomass burning, a 14-yr long H_2 emission record is available from GFED3, showing considerable temporal variability (Fig. 5a). Here we test our conversions from the EDGAR and GFED3 CO and CH_4 emission inventories to H_2 emissions using the earlier discussed molar ratios of 0.25 for H_2/CO and 3.6 for H_2/CH_4. The comparison of the GFED3 CH_4-derived H_2 emissions with its H_2 emissions show a generally good agreement and is to some degree a confirmation of using CH_4 as a proxy for H_2 in biomass combustion processes (Fig. 5a). However, there is also some degree of circular conclusion in this comparison because some of the data (e.g. Cofer III et al., 1989, 1990, 1996; Ward et al., 1992), which we have used in our derivation of $\Delta H_2/\Delta CH_4$, are also indirectly used in GFED3 (van der Werf et al., 2010)

through the analysis of emission factors (Andreae and Merlet (2001) and updates), which partially draw on the same dry matter combustion estimates. The CO-derived H_2 emissions are generally lower compared to the CH_4-derived H_2 emissions for both GFED3 and EDGAR data sets. Where common records are available, the EDGAR CO and CH_4 emissions are considerably larger (30 to 40 %) than the respective GFED3 emissions, as are consequently the corresponding H_2 emissions. This discrepancy may be caused by EDGAR adopting older GFED version 2 values (IEA, 2011), which are significantly higher than GFED3 (T. T. Van Leeuwen, personal communication, 2011).

The GFED3 biomass burning H_2 emission estimates are significantly lower (except for the record year 1997) compared to the global H_2 emissions estimate from biomass burning by Laursen et al. (1992) of 21 Tg for an unspecified year. Our molar H_2/CH_4 ratio of 3.6 is also smaller compared to the ratio of 4.3 by Laursen et al. (1992), which we calculate from their H_2 and CH_4 emission estimates.

The scaling of H_2 emissions to the CO emissions for biomass burning has been performed in earlier studies with somewhat different ratios and CO emission inventories but yielding similar results, e.g. the study by Price et al. (2007). To our knowledge, this is the first time that H_2 emissions are scaled to CH_4 emissions using H_2/CH_4 ratios.

The combined emissions from biomass and biofuel H_2 combustion are at the lower end of the range found in the literature (Table 1), and the combined estimate of 8.4 ± 1.6 Tg from 2000 is the lowest ever reported for this category.

4 Conclusions

Our study has attempted to fill some of the gaps in the knowledge of H_2 emissions quantification from fossil fuel and biomass combustion. The low H_2/CO from residential combustion processes should lead to a total urban H_2/CO ratio lower than the traffic-related ratio. This "dilution" effect would presumably be seasonal, as heating systems are more strongly used during winter time. Thus, such an effect should be seen in multi-annual urban data records if CO emissions from heating are of similar magnitude as those from traffic. Even though there is evidence in the literature (Hammer et al., 2009; Aalto et al., 2009; Yver et al., 2009) for lower winter H_2/CO ratios compared to summers, a careful detailed analysis is beyond the scope of this paper. In a similar manner, the low diesel exhaust H_2/CO ratio (roughly 1/20th of the gasoline exhaust ratio) has a "diluting" effect on the overall gasoline-dominated ratio. However, because the absolute H_2 and CO emissions from a diesel engine are much smaller than those from a gasoline engine, it would require a very large diesel fraction of a vehicle fleet to significantly affect the gasoline-dominated fleet ratio.

It remains to be investigated to what extent our findings of negligible H_2 emissions from oil and gas burners are applicable for similar burner/heater systems in other parts of the world. Our results suggest that the heater system (oil vs. natural gas) or the age and design are not of prime relevance, but mainly how well the burner is tuned. As for the low H_2 emissions from our sampled waste incinerator plants, these results are unlikely to be applicable to less controlled incineration of waste, particularly in landfills. Our analysis also reveals the lack of knowledge on H_2 emissions from coal combustion (particularly from power plants), which could potentially be a significant fossil fuel combustion source of H_2. This may be one explanation for our estimated fossil fuel H_2 emissions being considerably smaller compared to those by e.g. Yver et al. (2011) and Ehhalt and Rohrer (2009).

Our surprising findings of a lack of H_2 emissions in the presence of CO emissions, and the isotopic hydrogen signatures of fossil fuel heater exhausts suggest that our understanding of the H_2 and CO involvement in these combustion processes is incomplete. More process studies involving quantification of H_2O, along with isotope analysis on the main H and C-containing compounds may help in this regard. Combustion experiments with controlled (including zero) H_2 mole fractions and isotope signatures in the advected air could help to better understand the exhaust H_2 characteristics of fossil fuel burner systems with low emissions.

Supplementary material related to this article is available online at: http://www.atmos-chem-phys.net/12/6275/2012/acp-12-6275-2012-supplement.pdf.

Acknowledgements. We acknowledge all owners and managers of the sampled heating and incinerator systems for access to their buildings and for their generous support. Kerstin Zeyer and Peter Honegger conducted some of the waste incinerator sampling and Robert Alvarez contributed to the diesel exhaust experiments. Christoph Zellweger provided support in CO calibration and measurements. Matthias Hill and Angelina Wenger provided technical assistance. Peter Salameh provided support with the chromatography software and the data processing. This study was also carried out under the auspices of EuroHydros (European Commission FP 6, Priority Global Change and Ecosystems) and the project "Transition to Hydrogen-Based Transportation" of the Swiss Competence Center Energy and Mobility (CCEM-CH). S. Walter was supported by the project "H_2 budget" of the Dutch national science foundation NWO (grant 816-01-001).

Edited by: M. Heimann

References

Aalto, T., Lallo, M., Hatakka, J., and Laurila, T.: Atmospheric hydrogen variations and traffic emissions at an urban site in Finland, Atmos. Chem. Phys., 9, 7387–7396, doi:10.5194/acp-9-7387-2009, 2009.

Andreae, M. O. and Merlet, P.: Emission of trace gases and aerosols from biomass burning, Global Biogeochem. Cy., 15, 955–966, 2001.

Batenburg, A. M., Walter, S., Pieterse, G., Levin, I., Schmidt, M., Jordan, A., Hammer, S., Yver, C., and Röckmann, T.: Temporal and spatial variability of the stable isotopic composition of atmospheric molecular hydrogen: observations at six EUROHYDROS stations, Atmos. Chem. Phys., 11, 6985–6999, doi:10.5194/acp-11-6985-2011, 2011.

Bond, S. W.: Atmospheric Abundance and Anthropogenic Sources of Molecular Hydrogen: Status and Outlook Towards a H_2-intensive Economy, Ph.D. Thesis, Swiss Federal Institute of Technology, Zurich, No. 19346, 2010.

Bond, S. W., Alvarez, R., Vollmer, M. K., Steinbacher, M., Weilenmann, M., and Reimann, S.: Molecular hydrogen (H_2) emissions from gasoline and diesel vehicles, Sci. Total Environ., 408, 3596–3606, doi:10.1016/j.scitotenv.2010.04.055, 2010.

Bond, S. W., Gül, T., Reimann, S., Buchmann, B., and Wokaun, A.: Emissions of anthropogenic hydrogen to the atmosphere during the potential transition to an increasingly H_2-intensive economy, Int. J. Hydrogen Energ, 36, 1122–1135, doi:10.1016/j.ijhydene.2010.10.016, 2011a.

Bond, S. W., Vollmer, M. K., Steinbacher, M., Henne, S., and Reimann, S.: Atmospheric molecular hydrogen (H_2): observations at the high-altitude site Jungfraujoch, Switzerland, Tellus B., 63, 64–76, doi:10.1111/j.1600-0889.2010.00509.x, 2011b.

Cofer III, W. R., Levine, J. S., Sebacher, D. I., Winstead, E. L., Riggan, P. J., Stocks, B. J., Brass, J. A., Ambrosia, V. G., and Boston, P. J.: Trace gas emissions from chaparral and boreal forest fires, J. Geophys. Res., 94, 2255–2259, 1989.

Cofer III, W. R., Levine, J. S., Winstead, E. L., LeBel, P. J., Koller Jr, A. M., and Hinkle, C. R.: Trace gas emissions from burning Florida wetlands, J. Geophys. Res., 95, 1865–1870, 1990.

Cofer III, W. R., Levine, J. S., Winstead, E. L., Cahoon, D. R., Sebacher, D. I., Pinto, J. P., and Stocks, B. J.: Source composition of trace gases released during African savanna fires, J. Geophys. Res., 101, 23597–23602, 1996.

Craig, H.: Standards for reporting concentrations of deuterium and oxygen-18 in natural waters, Science, 133, 1833–1834, 1961.

Crutzen, P. J. Heidt, L. E., Krasnec, J. P., Pollock, W. H., and Seiler, W.: Biomass burning as a source of atmospheric gases CO, H_2, N_2O, NO, CH_3Cl and COS, Nature, 282, 253–256, 1979.

Derendorp, L., Quist, J. B., Holzinger, R., and Röckmann, T.: Emissions of H_2 and CO from leaf litter of Sequoiadendron giganteum, and their dependence on UV radiation and temperature, Atmos. Environ., 45, 7520–7524, doi:10.1016/j.atmosenv.2011.09.044, 2011.

Dlugokencky, E. J., Myers, R. C., Lang, P. M., Masarie, K. A., Crotwell, A. M., Thoning, K. W., Hall, B. D., Elkins, J. W., and Steele, L. P.: Conversion of NOAA atmospheric dry air CH_4 mole fractions to a gravimetrically prepared standard scale, J. Geophys. Res., 110, D18306, doi:10.1029/2005JD006035, 2005.

Duncan, B. N., Logan, J. A., Bey, I., Megretskaia, I. A., Yantosca, R. M., Novelli, P. C., Jones, N. B., and Rinsland, C. P.: Gobal budget of CO, 1988–1997: Source estimates and validation with a global model, J. Geophys. Res., 112, D22301, doi:10.1029/2007JD008459, 2007.

Ehhalt, D. H. and Rohrer, F.: The tropospheric cycle of H_2: a critical review, Tellus, Ser. B., 61, 500–535, doi:10.1111/j.1600-0889.2009.00416.x, 2009.

Ehhalt, D. H., Davidson, J. A., Cantrell, C. A., Friedman, I., and Tyler, S.: The kinetic isotope effect in the reaction of H_2 with OH, J. Geophys. Res., 94, 9831–9836, 1989.

Feilberg, K. L., Johnson, M. S., Bacak, A., Röckmann, T., and Nielsen, C. J.: Relative tropospheric photolysis rates of HCHO and HCDO measured at the European photoreactor facility, J. Phys. Chem. A, 111, 9034–9046, doi:10.1021/jp070185x, 2007.

Fulton, L. and Eads, G.: IEA/SMP model documentation and reference case projection, auxilliary material to: Mobility 2030: Meeting the challenges to sustainability; the Sustainable Mobility Project, IEA/CRA, 2004.

Gerst, S. and Quay, P.: Deuterium component of the global molecular hydrogen cycle, J. Geophys. Res., 106, 5021–5031, 2001.

Giglio, L., Randerson, J. T., van der Werf, G. R., Kasibhatla, P. S., Collatz, G. J., Morton, D. C., and DeFries, R. S.: Assessing variability and long-term trends in burned area by merging multiple satellite fire products, Biogeosciences, 7, 1171–1186, doi:10.5194/bg-7-1171-2010, 2010.

Gonfiantini, R.: Standards for stable isotope measurements in natural compounds, Nature, 271, 534–536, 1978.

Grant, A., Stanley, K. F., Henshaw, S. J., Shallcross, D. E., and O'Doherty, S.: High-frequency urban measurements of molecular hydrogen and carbon monoxide in the United Kingdom, Atmos. Chem. Phys., 10, 4715–4724, doi:10.5194/acp-10-4715-2010, 2010a.

Grant, A., Witham, C. S., Simmonds, P. G., Manning, A. J., and O'Doherty, S.: A 15 year record of high-frequency, in situ measurements of hydrogen at Mace Head, Ireland, Atmos. Chem. Phys., 10, 1203–1214, doi:10.5194/acp-10-1203-2010, 2010b.

Hammer, S., Vogel, F., Kaul, M., and Levin, I.: The H_2/CO ratio of emissions from combustion sources: comparison of top-down with bottom-up measurements in southwest Germany, Tellus B., 61, 547–555, doi:10.1111/j.1600-0889.2009.00418.x, 2009.

Hauglustaine, D. A. and Ehhalt, D. H.: A three-dimensional model of molecular hydrogen in the troposphere, J. Geophys. Res., 107, 4330, doi:10.1029/2001JD001156, 2002.

IEA: CO_2 Emissions from Fuel Combustion, IEA Statistics, International Energy Agency, Paris, 2011.

Jordan, A. and Steinberg, B.: Calibration of atmospheric hydrogen measurements, Atmos. Meas. Tech., 4, 509–521, doi:10.5194/amt-4-509-2011, 2011.

Laursen, K. K., Hobbs, P. V., Radke, L. F., and Rasmussen, R. A.: Some trace gas emissions from North American biomass fires with an assessment of regional and global fluxes from biomass burning, J. Geophys. Res., 97, 20687–20701, 1992.

Lee, H., Rahn, T., and Throop, H. L.: A novel source of atmospheric H_2: abiotic degradation of organic material, Biogeosciences Discuss., 9, 8641–8662, doi:10.5194/bgd-9-8641-2012, 2012.

Leippert, F., Kasser, F., and Heldstab, J.: Switzerland's Informative Inventory Report 2010 (IIR); Submission under the UNECE Convention on Long-range Transboundary Air Pollution, Tech. Rep. Submission of March 2010 to the United Nations ECE Secretariat, INFRAS Consulting group, Zurich, for Federal Office

for the Environmennt (FOEN), Berne, Switzerland, 2010.

Mar, K. A., McCarthy, M. C., Connell, P., and Boering, K. A.: Modeling the photochemical origins of the extreme deuterium enrichtment in stratospheric H_2, J. Geophys. Res., 112, D19302, doi:10.1029/2006JD007403, 2007.

Mohn, J., Zeeman, M. J., Werner, R. A., Eugster, W., and Emmenegger, L.: Continuous field measurements of $\delta^{13}C$–CO_2 and trace gases by FTIR spectroscopy, Isot. Environ. Health. Stud., 44, 241–251, doi:10.1080/10256010802309731, 2008.

Nilsson, E. J. K., Johnson, M. S., Taketani, F., Matsumi, Y., Hurley, M. D., and Wallington, T. J.: Atmospheric deuterium fractionation: HCHO and HCDO yields in the $CH_2DO + O_2$ reaction, Atmos. Chem. Phys., 7, 5873–5881, doi:10.5194/acp-7-5873-2007, 2007.

Nilsson, E. J. K., Andersen, V. F., Skov, H., and Johnson, M. S.: Pressure dependence of the deuterium isotope effect in the photolysis of formaldehyde by ultraviolet light, Atmos. Chem. Phys., 10, 3455–3462, doi:10.5194/acp-10-3455-2010, 2010.

Novelli, P. C., Lang, P. M., Masarie, K. A., Hurst, D. F., Myers, R., and Elkins, J. W.: Molecular hydrogen in the troposphere: global distribution and budget, J. Geophys. Res., 104, 30427–30444, 1999.

Olivier, J. G. J., Berdowski, J. J. M., Peter, J. A. H. W., Bakker, J., Visschedijk, A. J. H., and Bloos, J. P. J.: Applications of EDGAR emission database for global atmospheric research, Tech. Rep. RIVM report no. 773301001; NOP report no. 410200051, RIVM, Bilthoven, The Netherlands, 2002.

Pieterse, G., Krol, M. C., Batenburg, A. M., Steele, L. P., Krummel, P. B., Langenfelds, R. L., and Röckmann, T.: Global modelling of H_2 mixing ratios and isotopic compositions with the TM5 model, Atmos. Chem. Phys., 11, 7001–7026, doi:10.5194/acp-11-7001-2011, 2011.

Popa, M. E., Vermeulen, A. T., van den Bulk, W. C. M., Jongejan, P. A. C., Batenburg, A. M., Zahorowski, W., and Röckmann, T.: H_2 vertical profiles in the continental boundary layer: measurements at the Cabauw tall tower in The Netherlands, Atmos. Chem. Phys., 11, 6425–6443, doi:10.5194/acp-11-6425-2011, 2011.

Price, H., Jaeglé, L., Rice, A., Quay, P., Novelli, P. C., and Gammon, R.: Global budget of molecular hydrogen and its deuterium content: Constraints from ground station, cruise, and aircraft observations, J. Geophys. Res., 112, D22108, doi:10.1029/2006JD008152, 2007.

Rahn, T., Eiler, J. M., Kitchen, N., Fessenden, J. E., and Randerson, J. T.: Concentration and deltaD of molecular hydrogen in boreal forests: Ecosystem-scale systematics of atmospheric H_2, Geophys. Res. Lett., 29, 1888, doi:10.1029/2002GL015118, 2002a.

Rahn, T., Kitchen, N., and Eiler, J.: D/H ratios of atmospheric H_2 in urban air: Results using new methods for analysis of nanomolar H_2 samples, Geochim. Cosmochim. Acta, 66, 2475–2481, 2002b.

Rahn, T., Eiler, J. M., Boering, K. A., Wennberg, P. O., McCarthy, M. C., Tyler, S., Schauffler, S., Donnelly, S., and Atlas, E.: Extreme deuterium enrichment in stratospheric hydrogen and the global atmospheric budget of H_2, Nature, 424, 918–921, 2003.

Rhee, T. S., Mak, J., Röckmann, T., and Brenninkmeijer, C. A. M.: Continuous-flow isotope analysis of the deuterium/hydrogen ratio in atmospheric hydrogen, Rapid Commun. Mass Spectrom, 18, 299–306, 2004.

Rhee, T. S., Brenninkmeijer, C. A. M., Braß, M., and Brühl, C.: Isotopic composition of H_2 from CH_4 oxidation in the stratosphere and the troposphere, J. Geophys. Res., 111, D23303, doi:10.1029/2005JD006760, 2006a.

Rhee, T. S., Brenninkmeijer, C. A. M., and Röckmann, T.: The overwhelming role of soils in the global atmospheric hydrogen cycle, Atmos. Chem. Phys., 6, 1611–1625, doi:10.5194/acp-6-1611-2006, 2006b.

Rice, A., Quay, P., Stutsman, J., Gammon, R., Price, H., and Jaeglé, L.: Meridional distribution of molecular hydrogen and its deuterium content in the atmosphere, J. Geophys. Res., 115, D12306, doi:10.1029/2009JD012529, 2010.

Röckmann, T., Rhee, T. S., and Engel, A.: Heavy hydrogen in the stratosphere, Atmos. Chem. Phys., 3, 2015–2023, doi:10.5194/acp-3-2015-2003, 2003.

Röckmann, T., Gómez Álvarez, C. X., Walter, S., van der Veen, C., Wollny, A. G., Gunthe, S. S., Helas, G., Pöschl, U., Keppler, F., Greule, M., and Brand, W. A.: Isotopic composition of H_2 from biomass burning dependence on combustion efficiency, moisture content and δD of local precipitation, J. Geophys. Res., 115, D17308, doi:10.1029/2009JD013188, 2010a.

Röckmann, T., Walter, S., Bohn, B., Wegener, R., Spahn, H., Brauers, T., Tillmann, R., Schlosser, E., Koppmann, R., and Rohrer, F.: Isotope effect in the formation of H_2 from H_2CO studied at the atmospheric simulation chamber SAPHIR, Atmos. Chem. Phys., 10, 5343–5357, doi:10.5194/acp-10-5343-2010, 2010b.

Sander, S. P., Friedl, R. R., Ravishankara, A. R., Golden, D. M., Kolb, C. E., Kurylo, M. J., Molina, M. J., Moortgat, G. K., Keller-Rudek, H., Finlayson-Pitts, B. J., Wine, P. H., Huie, R. E., and Orkin, V. L.: Chemical Kinetics and Photochemical Data for Use in Atmospheric Studies, Evaluation Number 15 of the NASA Panel for Data Evaluation, JPL Publication 06-2, Jet Propulsion Laboratory, Pasadena, 2006.

Sanderson, M. G., Collins, W. J., Derwent, R. G., and Johnson, C. E.: Simulation of global hydrogen levels using a Lagrangian three-dimensional model, J. Atmos. Chem., 46, 15–28, 2003.

Schimmelmann, A., Sessions, A. L., and Mastalerz, M.: Hydrogen isotopic (D/H) composition of organic matter during diagenesis and thermal maturation, Annual Review of Earth and Planetary Sciences, 34, 501–533, doi:10.1146/annurev.earth.34.031405.125011, 2006.

Schultz, M. G., Diehl, T., Brasseur, G. P., and Zittel, W.: Air pollution and climate-forcing impacts of a global hydrogen economy, Science, 302, 624–627, 2003.

Shi, B. and Jin, C.: Inverse kinetic isotope effects and deuterium enrichment as a function of carbon number during formation of C-C bonds in cobalt catalyzed Fischer-Tropsch synthesis, Appl. Catal. A: Gen, 393, 178–183, doi:10.1016/j.apcata.2010.11.039, 2011.

Simmonds, P. G., Derwent, R. G., O'Doherty, S., Ryall, D. B., Steele, L. P., Langenfelds, R. L., Salameh, P., Wang, H. J., Dimmer, C. H., and Hudson, L. E.: Continuous high-frequency observations of hydrogen at the Mace Head baseline atmospheric monitoring station over the 1994–1998 period, J. Geophys. Res., 105, 12105–12121, 2000.

Steinbacher, M., Fischer, A., Vollmer, M. K., Buchmann, B., Reimann, S., and Hueglin, C.: Perennial observations of molecular hydrogen (H_2) at a suburban site in Switzerland, Atmos. Envi-

ron., 41, 2111–2124, doi:10.1016/j.atmosenv.2006.10.075, 2007.

Talukdar, R. K., Gierczak, T., Goldfarb, L., Rudich, Y., Madhava Rao, B. S., and Ravishankara, A. R.: Kinetics of hydroxyl radical reactions with isotopically labeled hydrogen, J. Phys. Chem., 100, 3037–3043, 1996.

van der Werf, G. R., Randerson, J. T., Giglio, L., Collatz, G. J., Mu, M., Kasibhatla, P. S., Morton, D. C., DeFries, R. S., Jin, Y., and van Leeuwen, T. T.: Global fire emissions and the contribution of deforestation, savanna, forest, agricultural, and peat fires (1997–2009), Atmos. Chem. Phys., 10, 11707–11735, doi:10.5194/acp-10-11707-2010, 2010.

Vogel, B., Feck, T., Grooß, J.-U., and Riese, M.: Impact of a possible future global hydrogen economy on Arctic stratospheric ozone loss, Energy Environ. Sci., 5, 6445–6452, doi:10.1039/c2ee03181g, 2012.

Vollmer, M. K., Juergens, N., Steinbacher, M., Reimann, S., Weilenmann, M., and Buchmann, B.: Road vehicle emissions of molecular hydrogen (H_2) from a tunnel study, Atmos. Environ., 41, 8355–8369, doi:10.1016/j.atmosenv.2007.06.037, 2007.

Vollmer, M. K., Walter, S., Bond, S. W., Soltic, P., and Röckmann, T.: Molecular hydrogen (H_2) emissions and their isotopic signatures (H/D) from a motor vehicle: implications on atmospheric H_2, Atmos. Chem. Phys., 10, 5707–5718, doi:10.5194/acp-10-5707-2010, 2010.

Walter, S., Laukenmann, S., Stams, A. J. M., Vollmer, M. K., Gleixner, G., and Röckmann, T.: The stable isotopic signature of biologically produced molecular hydrogen (H_2), Biogeosciences Discuss., 8, 12521–12541, doi:10.5194/bgd-8-12521-2011, 2011.

Ward, D. E., Susott, R. A., Kauffman, J. B., Babbitt, R. E., Cummings, D. L., Dias, B., Holben, B. N., Kaufman, Y. J., Rasmussen, R. A., and Setzer, A. W.: Smoke and fire characteristics for cerrado and deforestation burns in Brazil: BASE-B experiment, J. Geophys. Res., 97, 14601–14619, 1992.

Warwick, N. J., Bekki, S., Nisbet, E. G., and Pule, J. A.: Impact of a hydrogen economy on the stratosphere and troposphere studied in a 2-D model, Geophys. Res. Lett., 31, L05107, doi:10.1029/2003GL019224, 2004.

Xiao, X., Prinn, R. G., Simmonds, P. G., Steele, L. P., Novelli, P. C., Huang, J., Langenfelds, R. L., O'Doherty, S., Krummel, P. B., Fraser, P. J., Porter, L. W., Weiss, R. F., Salameh, P., and Wang, R. H. J.: Optimal estimation of the soil uptake rate of molecular hydrogen from the Advanced Global Atmospheric Gases Experiment and other measurements, J. Geophys. Res., 112, D07303, doi:10.1029/2006JD007241, 2007.

Yevich, R. and Logan, J. A.: An assessment of biofuel use and burning of agricultural waste in the developing world, Global Biogeochem. Cy., 17, 1095, doi:10.1029/2002GB001952, 2003.

Yokelson, R. J., Crounse, J. D., DeCarlo, P. F., Karl, T., Urbanski, S., Atlas, E., Campos, T., Shinozuka, Y., Kapustin, V., Clarke, A. D., Weinheimer, A., Knapp, D. J., Montzka, D. D., Holloway, J., Weibring, P., Flocke, F., Zheng, W., Toohey, D., Wennberg, P. O., Wiedinmyer, C., Mauldin, L., Fried, A., Richter, D., Walega, J., Jimenez, J. L., Adachi, K., Buseck, P. R., Hall, S. R., and Shetter, R.: Emissions from biomass burning in the Yucatan, Atmos. Chem. Phys., 9, 5785–5812, doi:10.5194/acp-9-5785-2009, 2009.

Yokelson, R. J., Burling, I. R., Urbanski, S. P., Atlas, E. L., Adachi, K., Buseck, P. R., Wiedinmyer, C., Akagi, S. K., Toohey, D. W., and Wold, C. E.: Trace gas and particle emissions from open biomass burning in Mexico, Atmos. Chem. Phys., 11, 6787–6808, doi:10.5194/acp-11-6787-2011, 2011.

Yver, C., Schmidt, M., Bousquet, P., Zahorowski, W., and Ramonet, M.: Estimation of the molecular hydrogen soil uptake and traffic emissions at a suburban site near Paris through hydrogen, carbon monoxide, and radon-222 semicontinuous measurements, J. Geophys. Res., 114, D18304, doi:10.1029/2009JD012122, 2009.

Yver, C. E., Pison, I. C., Fortems-Cheiney, A., Schmidt, M., Chevallier, F., Ramonet, M., Jordan, A., Søvde, O. A., Engel, A., Fisher, R. E., Lowry, D., Nisbet, E. G., Levin, I., Hammer, S., Necki, J., Bartyzel, J., Reimann, S., Vollmer, M. K., Steinbacher, M., Aalto, T., Maione, M., Arduini, J., O'Doherty, S., Grant, A., Sturges, W. T., Forster, G. L., Lunder, C. R., Privalov, V., Paramonova, N., Werner, A., and Bousquet, P.: A new estimation of the recent tropospheric molecular hydrogen budget using atmospheric observations and variational inversion, Atmos. Chem. Phys., 11, 3375–3392, doi:10.5194/acp-11-3375-2011, 2011.

Zellweger, C., Hüglin, C., Klausen, J., Steinbacher, M., Vollmer, M., and Buchmann, B.: Inter-comparison of four different carbon monoxide measurement techniques and evaluation of the long-term carbon monoxide time series of Jungfraujoch, Atmos. Chem. Phys., 9, 3491–3503, doi:10.5194/acp-9-3491-2009, 2009.